Slovak University of Technology in Bratislava
Institute of Information Engineering, Automation, and Mathematics

PROCEEDINGS

of the 18th International Conference on Process Control

Hotel Titris, Tatranská Lomnica, Slovakia, June 14 – 17, 2011

ISBN 978-80-227-3517-9

http://www.kirp.chtf.stuba.sk/pc11

Editors: M. Fikar and M. Kvasnica

Bencic, G., Jelavić, M., Perić, N.: Application of Quantitative Feedback Theory for Wind Turbine Controller Design, Editors: Fikar, M., Kvasnica, M., In *Proceedings of the 18th International Conference on Process Control*, Tatranská Lomnica, Slovakia, 496–505, 2011.

Full paper online: http://www.kirp.chtf.stuba.sk/pc11/data/abstracts/057.html

Application of Quantitative Feedback Theory for Wind Turbine Controller Design

Goran Benčić*, Mate Jelavić, Nedjeljko Perić*****

** KONČAR – Power Plant and Electric Traction Engineering, Zagreb, Croatia*
(goran.bencic@koncar-ket.hr)

*** KONČAR – Electrical Engineering Institute, Zagreb, Croatia*
(mjelavic@koncar-institut.hr)

**** Faculty of Electrical Engineering and Computing, Zagreb, Croatia*
(nedjeljko.peric@fer.hr)

Abstract: *To enable wind turbines to produce power under great variety of wind conditions a sophisticated control system is needed. Wind turbine system is highly nonlinear and its dynamics changes rapidly with the change of wind speed. Many classical control methods fail to properly address this uncertainty of wind turbine dynamics. For that reason Quantitative Feedback Theory is presented and its application to synthesis of rotor speed controller.*

1. INTRODUCTION

Modern wind turbines have to operate in wide range of operating conditions determined primarily by wind speed. To make it possible for wind turbine to produce power in such a variety of operating conditions a sophisticated control system is needed that will account for changes in operating conditions and accompanying changes in wind turbine dynamics [1]. The power of air that moves at speed v_w over the area swept by turbine rotor of radius R is given by (1):

$$P_W = \frac{1}{2}\rho_{air} R^2 \pi v_w^3 \qquad (1)$$

where ρ_{air} is density of air. From expression (1) it is clear that wind energy increases rapidly with increase in wind speed. This results in two very different operation regions of wind turbine, each of them placing specific demands upon control system. During weak winds power contained in the wind is lower than the rated power output of wind turbine generator. Therefore, the main task of the control system in this region is to maximize wind turbine power output by maximizing wind energy capture. It can be shown [2] that for each value of wind speed energy conversion efficiency is maximal for only one particular value of rotor speed. Since modern wind turbines are connected to grid using AC-DC-AC frequency converters, generator frequency is decoupled from grid frequency which enables variable speed operation. Therefore it becomes possible to vary the rotor speed and to maintain optimal energy conversion during varying wind speeds. On the other hand, during strong winds power of the wind is greater than the rated power output of wind turbine generator. Therefore, the wind energy conversion has to be constrained in this region to assure generator operation without overloading. Very efficient method for constraining wind energy conversion is pitching the rotor blades around their longitudinal axis which deteriorates their aerodynamic efficiency and therefore only a part of wind energy is used for driving the generator.

The main task of wind turbine control system is to obtain continuous power production under operating conditions determined by various wind speeds. As turbine power is directly proportional to its speed, power control can be done by controlling turbine speed. The principle scheme of wind turbine speed control system is shown in Fig. 1.

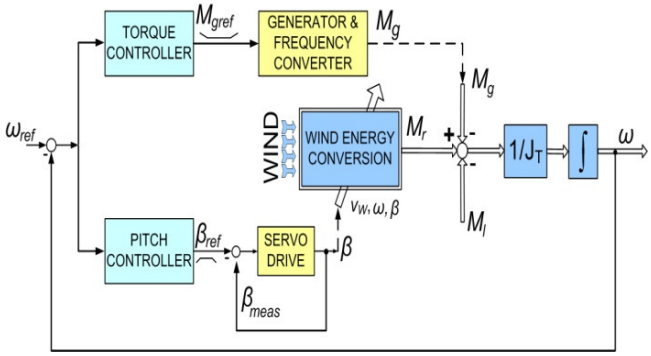

Fig. 1. Principle scheme of wind turbine control system [3]

As it can be seen in this figure turbine speed can be influenced and thus controlled by two means – by generator electromagnetic torque M_g which opposes rotor driving torque M_r and by pitch angle β which alters the wind energy conversion. For this reason turbine speed control system consists of two control loops: torque control loop and pitch control loop. Those control loops operate simultaneously but depending on operation region one of them is dominant. In the below rated operation region the torque control loop is used to control turbine speed to values that will result in maximal wind power capture. This control loop is not in the scope of this paper. Details on its specifics can be found in e.g. [3]. In the above rated region this control loop just holds generator torque at its rated value. The pitch control loop is used for setting the adequate pitch angle that will keep turbine speed at its reference value under all operating conditions determined by various winds. Below rated wind speed this loop sets pitch angle to value that assures maximal wind power capture which is usually around 0°. In this paper

we assume that all blades have the same pitch angle what is known as collective pitch. Controller in this loop, although used to control turbine speed, is commonly termed pitch controller. Blade positioning is mostly done using electrical servo drives that rotate blades by means of gearboxes and slewing rings. Position control of servo drives is usually achieved using frequency converters. This control loop design is rather simple and is not in the scope of the paper.

2. PROBLEMS OF CLASSICAL CONTROL SYSTEMS

The main problem for most of classical control methods is handling of nonlinear dynamical systems. Even simple models of wind turbines are highly nonlinear due to nature of aerodynamic conversion that takes place on all rotor blades. These models usually don't take into consideration aeroelasticity of the blades, wake effects, yaw errors, stall effect, tower shadow, wind shear effects etc. and still present a tough challenge for most of classical methods. The core of the problem mostly lies in inability of methods to explicitly account for uncertainty of process dynamical behavior that arises from changes in working conditions (higher wind speed, lower wind speed). Furthermore, when a controller is parametrized, there are usually no guarantees of stability and quality of disturbance rejection when operating point changes. For that reason it is necessary to perform extensive time simulations to a posteriori determine if initial specifications for stability and disturbance rejections are satisfied in all cases. QFT on the other hand rises up to this challenge as it can a priori process uncertainty, quantify it and used it in combination with closed loop specifications. It can also a priori guarantee fulfillment of closed loop specification.

3. MOTIVATION FOR UTILIZATION OF QFT

In the beginning of 1960s Horowitz introduced a new frequency domain based control method called Quantitative Feedback Theory (abbr. QFT) which presented a generalization of Bode's frequency domain work [4]. During Horowitz' involvement in the development of control system for Israeli battle aircrafts, QFT method was completed and received a form in which it is used today [4]. Successful utilization of QFT in aircraft control has proved the power of the method and enabled its application in helicopter control systems. When one takes into consideration that much of wind turbine aerodynamical modelling stems directly from helicopter aerodynamical modelling, it is only logical to conclude that QFT should handle in a satisfying manner control of rotor speed above rated wind speed. The main characteristic of QFT is the ability to explicitly take into account uncertainty of process that is to be controlled, and use this knowledge to develop a controller able to meet certain specifications (i.e. for efficient disturbance rejection, noise reduction, etc.). Due to high transparency of the method it is possible to surveil almost every aspect of the problem in hand and thus make needed trade-offs between quality of disturbance rejection, amount of stability margins, controller complexity and bandwidth utilization. This feature is especially appealing as it enables engineers to synthesize efficient low-bandwidth linear controllers of low order. Utilization of low-bandwidth controllers decreases system's sensitivity to noise and unmodelled dynamics. QFT is a completely rounded control method as it is applicable to various control systems: linear, nonlinear, time (non)varying, continuous and discrete, (non)minimum phased, Multiple Input Single Output (abbr. MISO), Multiple Input Multiple Output (abbr. MIMO), with output and state signals feedback, time-delayed (variant of QFT Smith predictor was developed for this purpose) [5]. It is even applicable to certain class of uncertain distributed systems whose behavior is described with partial differential equations (i.e. control of large scale manipulators) [5].

4. MISO QFT

The basis of all QFT methods (all variants of MIMO QFT, discrete QFT, QFT for non-minimum phased systems) is comprised in 2-degree of freedom structure called MISO QFT [5] shown in Fig. 2.

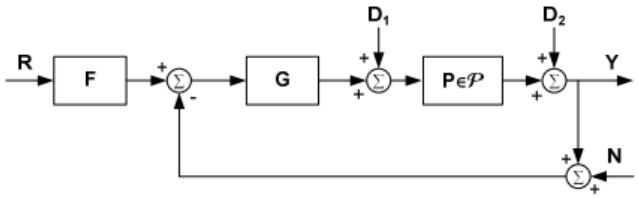

Fig. 2. MISO QFT control structure

The elements in Fig. 2 are described below:

$\mathcal{P}$ – a set of transfer functions where $P_i(j\omega) \in \mathcal{P}$ describing the area of process parametric uncertainty.

G – QFT controller intended to make this feedback system robust, reject disturbances and reduce sensitivity to noise.

F – prefilter that enables quality tracking of reference signal R.

Signals in Fig. 2 are: measurement noise N, disturbance D_1 on process P input, disturbance D_2 on process P output, reference signal R.

The process of obtaining an adequate QFT controller $G(s)$ and prefilter $F(s)$ can be described through following steps:

1) Determine the set of transfer functions $\mathcal{P} = \{P_i(j\omega_i)\}$ that describe the whole range of process dynamical behavior.
2) Choose a nominal process $P_0(j\omega)$ from the given set $\mathcal{P}$ (any one will do).
3) Choose discrete frequency set $\Omega = \{\omega_1, \omega_2, \dots, \omega_M\}$ from frequency range relevant for control. Further controller synthesis is performed on this discrete set Ω.
4) Generate templates (sets that describe area of phase vs amplitude variations) for every frequency from Ω. In other words, if phase and amplitude values are calculated for every $P_i \in \mathcal{P}$ for certain frequency $\omega_k \in \Omega$, then this set of values is called the template $\Pi(j\omega_k)$.

5) Determine a set of specification for closed loop system behavior (i.e. allowable upper and lower boundary for tracking of R, upper boundary for disturbance rejection, stability, control effort, etc.) and translate them to frequency domain.

6) Using Nichols chart, given specifications and templates, find frequency boundaries $\mathcal{B}_i$ on Nichols chart. For every specification there is a set of boundaries $\mathcal{B}_i$ generated on Nichols chart. This set is calculated only for frequencies from Ω. For example, $\mathcal{B}_i(j\omega_k)$ would present a boundary for i-th specification evaluated on ω_k. Crucial detail of this algorithm is that all of these boundaries are calculated in dependence of before mentioned nominal process $P_0(j\omega)$.

7) Draw the nominal open loop $L_0(j\omega) = P_0(j\omega)\,G(j\omega)$ on the same Nichols chart and commence with classical loop shaping procedures in order to satisfy calculated boundaries.

8) Draw the whole set of closed loop transfer functions on Bode diagram and find suitable prefilter F to satisfy servo specifications (if such exist) for tracking of reference R signal.

9) Perform frequency and time validation of control design. Iterate if necessary.

Step 6) is crucial for QFT method and will be explained in a graphical manner which could offer the reader a better insight. For example, a stability margin specification is given as (2):

$$\left|\frac{L(j\omega)}{1+L(j\omega)}\right| \le M_m \qquad (2)$$

This relation is represented as exterior of a red closed curve around the critical point (-180°, 0 dB) on Nichols chart on Fig. 3.

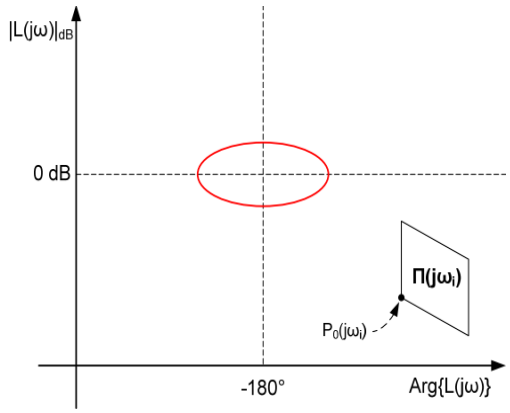

Fig. 3. Closed curve around critical point and the template $\Pi(j\omega_i)$

$\Pi(j\omega_i)$ represents the process template and $P_0(j\omega_i)$ represents the nominal process. The template needs to remain outside the region enclosed by the red curve. Firstly the template needs to be moved maximally close to the red curve (none of the points belonging to the template are allowed to enter the enclosed region) and the position of the nominal process need to be marked for every position of the template. Such movement of the template in magnitude-phase plane (Nichols chart) is possible if controller is connected as it enables adjustment of phase and magnitude i.e. translation Connect these markings of the nominal process (green line in Fig.4.). This green line actually represents the stability boundary $\mathcal{B}_s(j\omega_i)$ on frequency ω_i. If during step 7) the value of open loop transfer function $L_0(j\omega_i)$ remains outside the $\mathcal{B}_s(j\omega_i)$, then there is a guarantee that none of all possible closed loop systems values on ω_i will be within forbidden enclosed area. Similar graphical logic applies to other types of specifications. QFT software tools handle boundary generations by extracting template boundary (thus reducing the computation burden due to many insignificant interior points) and then solving systems of quadratic inequalities. The controller synthesis is finally performed on a set of resultant boundaries that represent the intersection of all boundaries.

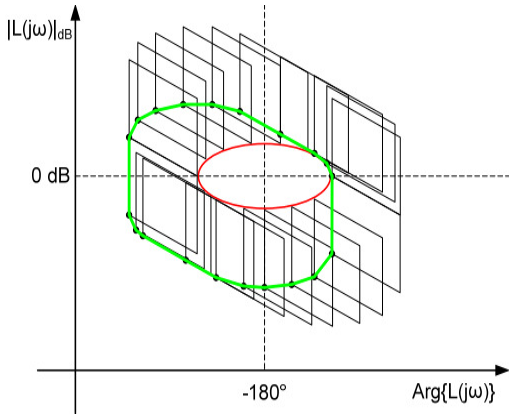

Fig. 4. Template moved around the curve forming a stability boundary $\mathcal{B}_s(j\omega_i)$

5. WIND TURBINE MODELLING

The first step in control system design is to obtain a suitable process model to describe dynamical behavior of wind turbine. Combination of blade element and momentum theory yields quite satisfactory description of wind turbine aerodynamic effects which are at center of scope in modelling. It is primarily utilized in simulation tools but lacks simplicity in order to be suitably used in the process of controller design due to iterative nature of the method. For this reason a different, more analytical, approach is used that develops a simplified mathematical model usual in the literature dealing with controller design. It will be described briefly, while the details on it can be found in [6] and [7].

Wind power P_w, given by expression (1), can never be completely transformed into wind turbine power P_{wt} and afterwards into electrical power P_{el}. The amount of wind power that is converted into turbine power P_{wt} can be described by expression (3):

$$P_{wt} = P_w C_p \qquad (3)$$

where C_p represents a performance coefficient.

The theoretical maximum for C_P is determined by the Betz' law [2] and equals $16/27 \approx 0.59$. The interesting part about

assumptions made in deriving Betz' law is that no particular turbine design was considered and no additional losses were included (wake losses, friction losses, etc.) which means that $16/27$ is an absolute limit for power extraction process. Modern wind turbines reach at best performance coefficient of 0.5. The value of C_P varies in dependence on wind speed v_w, rotor speed ω and blade pitch angle β. Wind speed and rotor tip speed are usually bound together introducing parameter λ that is called tip speed ratio [2] given by expression:

$$\lambda = \frac{\omega R}{v_w} \tag{4}$$

Typical dependence of performance coefficient upon tip speed ratio with pitch angle used as a parameter is shown in Fig. 5.

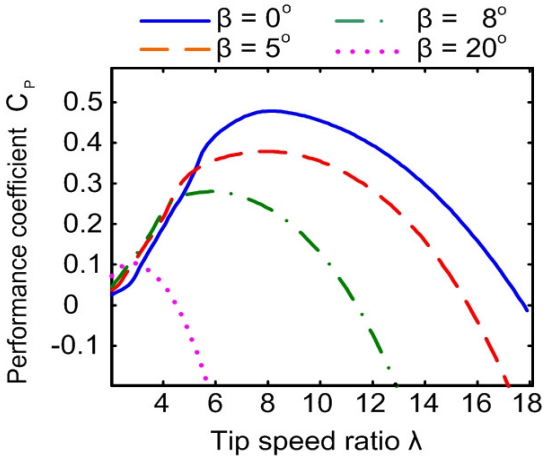

Fig. 5. Performance coefficient as a function of tip speed ratio [1]

Aerodynamic torque that drives wind turbine rotor is given by (5):

$$M_r = \frac{P_r}{\omega} = \frac{1}{2}\frac{\rho_{air} R^2 \pi v_w^3 C_p(\lambda,\beta)}{\omega} \tag{5}$$

Using relation defined by (4) a rearrangement of expression (5) is obtained as follows (6):

$$M_r = \frac{1}{2}\frac{\rho_{air} R^3 \pi v_w^2 C_p(\lambda,\beta)}{\lambda} \tag{6}$$

A quotient of performance coefficient C_p and tip speed ratio λ forms a new dimensionless parameter known as torque coefficient C_Q [2]:

$$C_Q(\lambda,\beta) = \frac{C_p(\lambda,\beta)}{\lambda} \tag{7}$$

Now the rotor speed ω can easily be found using principle equation of motion given by :

$$J_t \frac{d\omega}{dt} = M_r - M_g - M_{loss} \tag{8}$$

where M_g is generator electromagnetic torque, J_t is total moment of inertia of generator rotor and wind turbine, while M_{loss} is loss torque caused by friction losses (usually neglectable).

Wind turbine considered in this paper is In this paper we consider wind turbine with generator that is directly coupled with turbine rotor. This turbine setting known as direct drive system uses synchronous multipole generator that rotates at small speed of turbine rotor. Since rotor and generator speeds are the same no distinction between them is made throughout the paper. Because there is no gearbox between rotor and generator their moments of inertia can just be summed together in order to calculate total moment of inertia J_t. The coupling of rotor to the generator in direct drive solutions is very stiff and it can be considered as rigid thus removing any torsional oscillations what simplifies the control system design.

Before going further an important issue has to be addressed. Namely, expressions (5), (6) and (7) in this form would be valid only for structure with rigid tower and blades. In real situation the absolute wind speed v_w in mentioned expressions has to be replaced by wind speed that is "seen" by rotor blades. This wind speed seen by the rotor is the resultant of three factors: absolute wind speed v_w, speed of the tower movement perpendicular to wind speed (i.e. tower nodding speed) $\dot{x}_t$ and speed of blade movement perpendicular to wind speed (i.e. speed of blade flapwise movement). Influence of tower nodding on wind turbine control is much more pronounced than influence of blade flapwise movement. Therefore we focus only on tower nodding considering rotor blades as rigid. This results in a following expression describing the wind "seen" by rotor blades:

$$v_w^* = v_w - \dot{x}_t \tag{9}$$

Tower nodding originates from the fact that wind turbine tower is very lightly damped structure due to its great height (more than 100 meters in modern wind turbines) and need for moderate mass. To model the wind turbine tower precisely we would have to use model with distributed parameters and to describe it in terms of mass and stiffness distribution. Such a model wouldn't be very suitable for controller design so it has to be substituted by model with concentrated parameters. This can be done using modal analysis that is very common tool in wind turbine analysis [1], [3]. It describes a complex oscillatory structure as a composition of several simple oscillatory systems each of them being described by means of mass, stiffness and damping. By this representation complex tower oscillations are seen as a sum of many simple oscillations characterized by their modal frequencies which are one of the most important structural properties of wind turbine. It has been shown in practice [5] that fairly good modeling of wind turbine tower nodding can be achieved using two modal frequencies (two modes). Since we are here primarily interested in building model suitable for controller design we use only the first modal frequency. The justification for this lies in the fact that for the turbine in scope second modal frequency is more than 6 times greater than the first modal frequency and therefore falls out of the controller frequency bandwidth.

By using only one modal frequency tower dynamics can be described as:

$$M\ddot{x}_t + Dx_t + C\dot{x}_t = F(t) \tag{10}$$

where M, D, and C are modal mass damping and stiffness respectively and $F(t)$ is the generalized force that is originated by wind and that causes wind turbine tower oscillations. Tower modal properties in expression (10) are related to first tower modal frequency ω_{0t} as follows [6]:

$$D = 2\zeta_t \omega_{0t} M$$
$$C = (\omega_{0t})^2 M \quad (11)$$

where ζ_t is structural damping. For steel structure structural damping is mostly set to 0.005 [6]. Modal mass M can be calculated as [2]:

$$M = \int_0^{h_t} m(h)\Phi(h)^2 dh \quad (12)$$

where h_t is the height of the tower, $m(h)$ is the mass distribution along the tower height and $\Phi(h)$ is the tower's first mode shape. Note that actual distribution of mass along the tower has to be modified in order to include mass of the rotor and the nacelle which is assumed to be concentrated at the tower top.

Driving force F is mostly the rotor thrust force F_t caused by the wind. It can be shown [6] that thrust force, similar to aerodynamic torque, depends on wind speed, rotor speed and pitch angle. So similarly to (6) it can be expressed as [6]:

$$F_t = \frac{1}{2}\rho_{air} R^2 \pi v_w^2 C_t(\lambda, \beta) \quad (13)$$

where C_t is the, so called, thrust coefficient.

Expressions (6), (8), (10) and (13) form the simplified nonlinear model of wind turbine that is used in the following sections for controller design. Model is summarized below taking into account the fact that wind speed seen by the rotor is a sum of wind speed and tower nodding speed:

$$J_t \frac{d\omega}{dt} = M_r - M_g - M_{loss}$$
$$M_r = \frac{1}{2}\rho_{air} R^3 \pi (v_w - \dot{x}_t)^2 C_Q(\lambda, \beta) \quad (14)$$
$$F_t = \frac{1}{2}\rho_{air} R^2 \pi (v_w - \dot{x}_t)^2 C_t(\lambda, \beta)$$
$$M\ddot{x}_t + Dx_t + C\dot{x}_t = F(t)$$

Torque and thrust coefficients C_q and C_t are usually provided by wind turbine blade manufacturers or can be calculated using professional simulation tools.

On Fig. 6. a block diagram depicts the simulation model of the wind turbine used to obtain results that follow. The central part of it is the aerodynamical model shown on Fig. 7. that implements equations (6) and (13) defining M_r and F_t. C_Q and C_t are represented by 2D look-up tables with pitch angle β and tip speed ratio λ as their input signals. Torque M_r and thrust force F_t represent resulting output signals. The control system of the pitch drive will not be addressed in this paper and can be approximated, for small reference pitch changes, in a satisfactory manner by 2nd order aperiodical system. In reality, pitch drive would use cascaded position and speed control loops that would have to overcome aerodynamic torque developed around the longitudinal blade axes, stiction and friction induced torques inside the blade bearings.

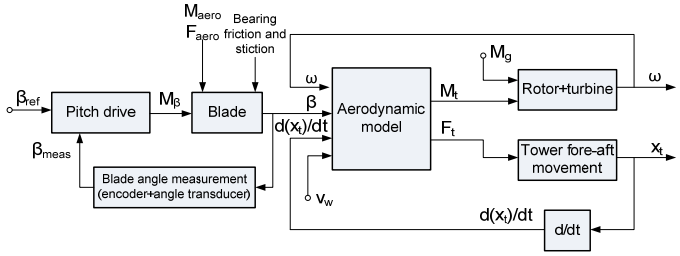

Fig. 6. Block diagram of the wind turbine simulation model

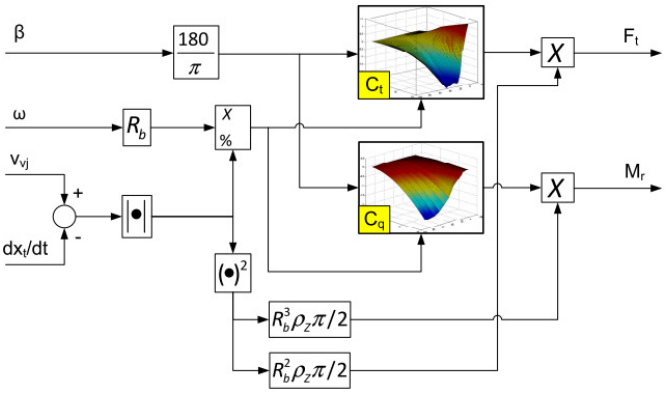

Fig. 7 Block diagram of aerodynamical model

In order to use QFT method for speed controller synthesis a linear model is required. From system of equations given by (14), second and third equation need to be linearized as shown below:

$$\Delta M_r = \left.\frac{\partial M_r}{\partial v_w}\right|_{O.P.} (\Delta v_w - \Delta \dot{x}_t) + \left.\frac{\partial M_r}{\partial \beta}\right|_{O.P.} \Delta\beta + \left.\frac{\partial M_r}{\partial \omega}\right|_{O.P.} \Delta\omega \quad (15)$$

$$\Delta F_t = \left.\frac{\partial F_t}{\partial v_w}\right|_{O.P.} (\Delta v_w - \Delta \dot{x}_t) + \left.\frac{\partial F_t}{\partial \beta}\right|_{O.P.} \Delta\beta + \left.\frac{\partial F_t}{\partial \omega}\right|_{O.P.} \Delta\omega \quad (16)$$

Term O.P. used in equations above is an abbreviation for operating point. An automated procedure was used in order to obtain partial derivatives in (15) and (16). Perturbation was introduced to stationary values of input signals and it was observed on output points in which extent these perturbations were amplified. Discrete wind range $\mathcal{V}_w$ was used to define operating points above rated wind speed (approximately 12 m/s):

$$\mathcal{V}_w = \{12,13,14,\ldots,24,25\}\ [m/s] \quad (17)$$

In this regime of operation it can be considered that constant nominal generator torque M_g is used, so no ΔMg is introduced into the system. Therefore this dynamics will be neglected. By combining linearized equations (15) and (16) with (8) and (10) an expression can be obtained that brings together into a classical relation pitch angle β (plant input) and wind speed v_w (disturbance input) with rotor speed ω (plant output):

$$\omega(s) = G(s)\beta(s) + G_d(s)v_w(s) \quad (18)$$

For every wind speed $v_{w,i} \in \mathcal{V}_w$ accompanying pair of transfer functions $G_i(s) \in \mathcal{G}$ and $G_{d,i}(s) \in \mathcal{G}_d$ is obtained.

Families $\mathcal{G}$ and $\mathcal{G}_d$ of transfer functions are shown on Fig. 8. and Fig. 9.

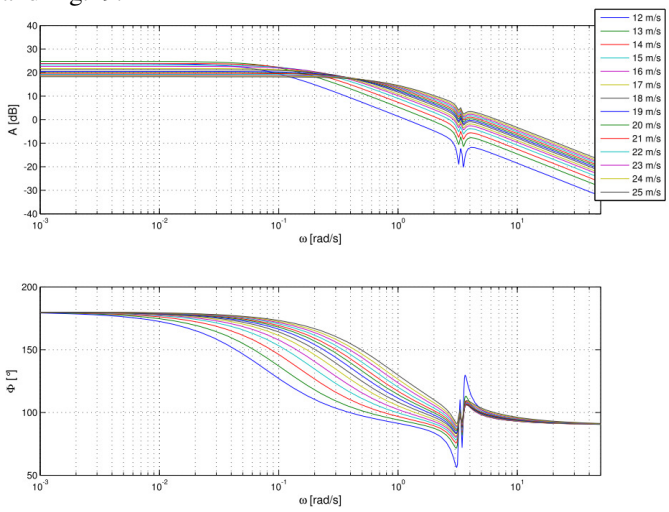

Fig. 8. Bode plot of transfer function family $\mathcal{G}$

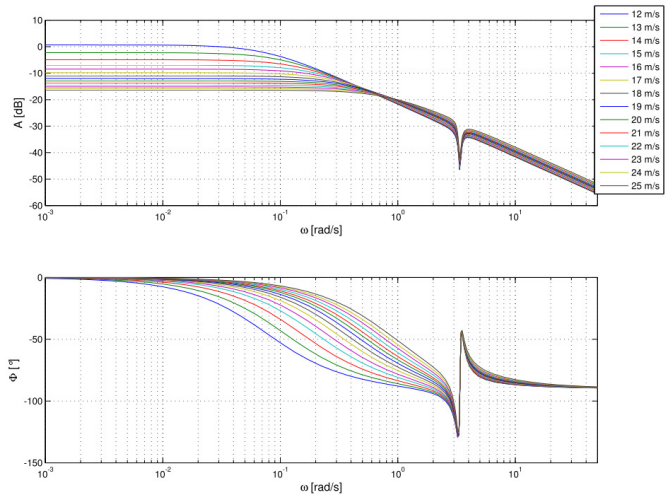

Fig. 9. Bode plot of transfer function family $\mathcal{G}_d$

Observe a phase shift on lower (relevant) frequency range by 180° on Fig. 8. that relates rotor speed change to pitch angle change. This means that a small rise in pitch angle produces negative change, due to phase shift, in rotor speed i.e. slowing down of the rotor. Physically this causes a decrease in angle of attack and consequently lowering of tangential forces on blade sections is caused. This in turn cumulatively decreases the value of driving torque M_r when contributions of all blades and all blade sections are summed.

6. DESIGN SPECIFICATIONS

Two types of specifications are defined and later on accompanying open loop boundaries on Nichols chart are calculated in order to facilitate controller design process. First appropriate discrete set of design frequencies needs to be specified. Regarding this problem there are no strict rules, instead some useful guidelines exist. Generally it is useful to choose frequencies that give results with meaningful differences in calculated boundaries. This can be computationally bothersome as it requires iterations. As a rule of thumb frequencies separated by an octave inside meaningful frequency range should suffice. Special care should be taken if process dynamics exhibits resonances at certain frequencies as then few frequencies around the resonance frequency should be chosen to appropriately describe abrupt phase and magnitude changes. Below is given the set Ω of frequencies that were used in calculations:

$$\Omega = \{10^{-3}, 10^{-2}, 10^{-1}, 0.5, 1, 2.5, 3.3, 3.38, 3.47, 5, 20\} \quad (19)$$

Due to natural frequency of tower first mode at $\omega_8 = 3.38\,rad/s$, nearby frequencies $\omega_7 = 3.3\,rad/s$ and $\omega_9 = 3.47\,rad/s$ were chosen. All the frequencies above $20\,rad/s$ are represented by $\omega_{11} = 20\,rad/s$ as their templates degenerate into virtually same shape that is solely dominated by variations of process magnitude. This can be stated as follows:

$$G(j\omega) \approx \frac{K}{(j\omega)^{\lambda}} \text{ when } \omega \gg \omega_b \quad (20)$$

where λ represents pole excess, ω_b represents bandwidth frequency and $K \in [K_{min}, K_{max}]$ represents amplitude variation. This fact is depicted on Fig. 10. by the template on $20\,rad/s$ that shows very small variations in phase values and dominant variations in amplitude values.

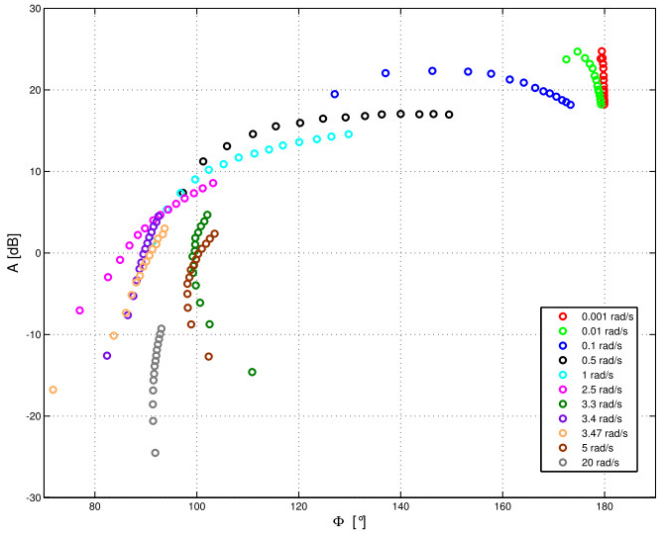

Fig. 10. Process templates representing variations of amplitude vs phase

First type of specifications refers to defining of stability margin factors. Instead of amplitude and phase margin, another relation was used that wraps them together stating (see expression (2)):

$$\left| \frac{C(j\omega)G_i(j\omega)}{1 + C(j\omega)G_i(j\omega)} \right| \leq M_m \; for \; \forall G_i \in \mathcal{G} \quad (21)$$

where $C(j\omega)$ represents controller transfer function. Amplitude margin (A.M.) and phase margin (P.M.) are bound together to M_m as follows:

$$A.M. = -20 \log\left(\frac{M_m}{1 + M_m}\right)$$
$$P.M. = 180° - \text{acos}\left(\frac{1}{2M_m^2} - 1\right) \quad (22)$$

Fig. 11 shows visually the meaning of relation (21) depicting A.M. and P.M. as extremes of amplitude and phase distance to critical point $(-180°,\ 0\ dB)$.

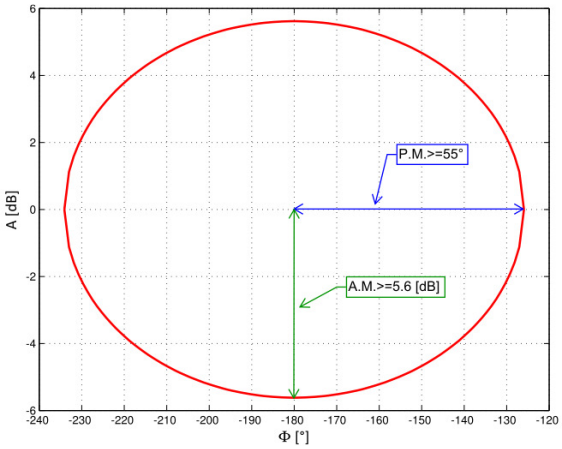

Fig. 11. Stability margin specifications on Nichols chart for $M_m = 1.1$

Second type of specifications refers to quality of disturbance compensation i.e. ability to maintain nominal rotation speed in spite of acting wind gust. Following relation needs to be satisfied:

$$\frac{\omega(s)}{v_w(s)} = \left|\frac{G_{d,i}(s)}{1 + G_i(s)C(s)}\right| \leq |G_{dist}(s)| \qquad (23)$$

for $\forall G_{d,i} \in \mathcal{G}_d$ and $\forall G_i \in \mathcal{G}$. $G_{dist}(s)$ is defined as:

$$G_{dist}(s) = \frac{1.8s^2 + 3.557s}{s^2 + 1.456s + 0.526} \qquad (24)$$

Unit step response and frequency amplitude characteristic of (24) is shown on Fig. 12.

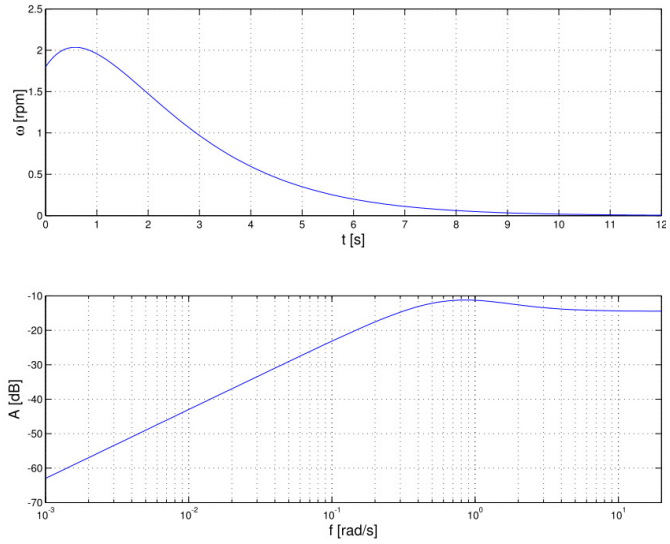

Fig. 12. Specified characteristic of response to unit step disturbance and accompanying frequency amplitude characteristic

There is no particular restriction on the initial part of the response which explains almost constant attenuation frequency characteristic in high frequency range. Namely, process response cannot suddenly jump at $t = 0\ s$ to certain value in a step like manner so there would be no point in defining any particular shape of response in initial period of time as this requires unnecessarily aggressive and complex controller design due to dominate high frequency design requests.

7. CONTROLLER DESIGN

Using defined specifications, discrete frequency set Ω and templates generated for $\forall\omega_i \in \Omega$ it possible to calculate, solving systems of quadratic inequalities, necessary stability and disturbance boundaries and depict their intersection (resultant boundaries) on Nichols chart.

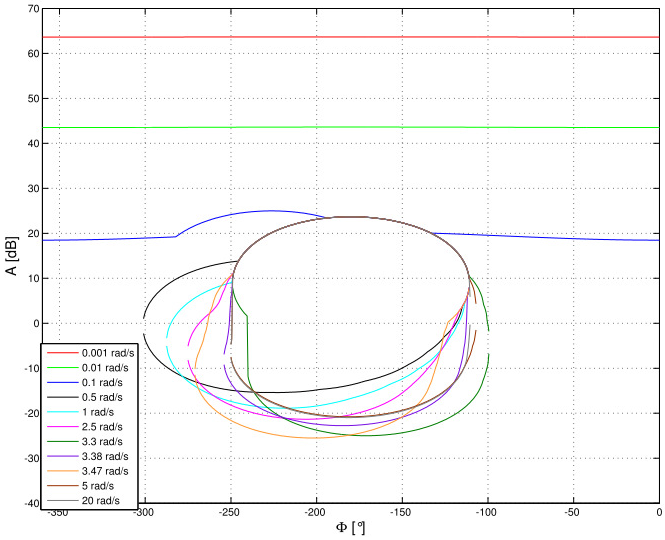

Fig. 13. Resultant boundaries on Nichols chart

A $12\ m/s$ linearized model was chosen as nominal plant process $G_0(s)$ so all the boundaries on Nichols chart were calculated in reference to this model. This in turn means that adequate loopshaping of open loop characteristic $L_0(s) = C(s)G_0(s)$ that satisfies given boundaries results in a fact that all closed/open loop characteristics satisfy accompanying closed/open loop characteristic. Controller transfer function is given as:

$$C(s) = -1.65\frac{(s + 0.5)(s + 1.4)}{s(s + 5)} \qquad (25)$$

On Fig. 14. it can be observed that point $\omega_4 = 0.5\ rad/s$ is not completely out of its boundary which was done on purpose as this would require movement of controller zero $z_1 = -0.5$ even closer to zero. This in turn weakens the integral action of the controller necessary for precision of stationary part of response as this zero would nearly cancel its action. Rise in complexity of the controller would be able to solve this issue but this is where QFT transparency comes handy as it enables us to make tradeoffs in controller design. It was also observed that neglecting of initial shape of response on Fig. 12 made the design easier with no evident loss in quality of response i.e. more simple controller was obtained that performs almost equally well. $z_2 = -1.4$ was inserted in order to obtain raise in the phase value of open loop so as to circumvent the round boundaries on their lower

right part. "Optimal" QFT controllers would have to minimize the cost of feedback, meaning that minimum of bandwidth should be utilized to satisfy given specifications. In order to gain such a controller points on nominal open loop characteristic $L_0(j\omega)$ should be maximally close to their boundary.

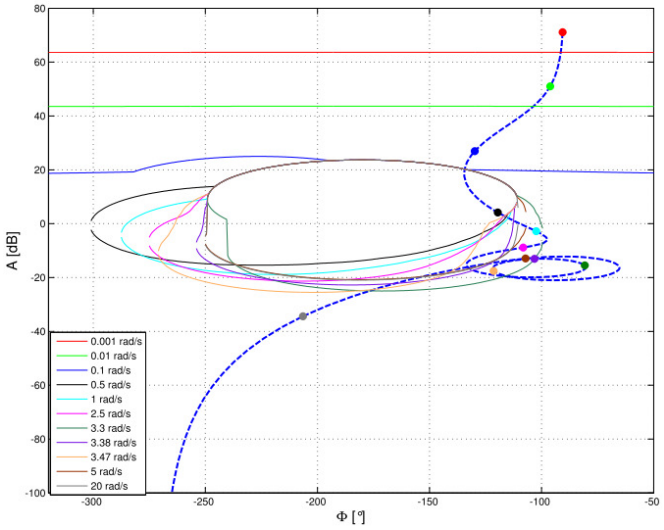

Fig. 14. Nominal open loop on Nichols chart vs calculated open loop boundaries

8. DESIGN VALIDATION

It remains to perform a validation of design by checking if for all family members prescribed specifications are satisfied. Fig. 15. shows validation of stability on all linear models.

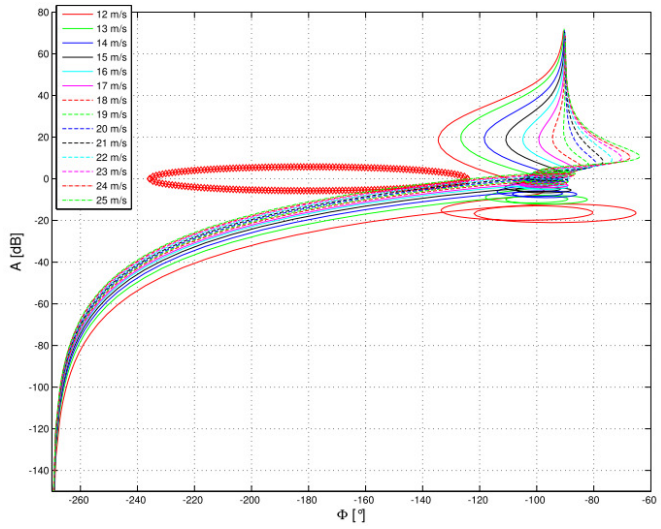

Fig. 15. Validation of stability specifications in frequency domain (boundary marked with red diamond markers)

Likewise Fig. 16. and Fig. 17. validate satisfactory behaviour in time and frequency domain of all linear models. Small ripple superimposed on rotor speed response stems from the fact that the tower top is oscillating towards/from the direction of wind meaning that relative wind speed v_w^* given by (9) is oscillatory changing. This in turn causes oscillatory changes in angle of attack of all blade sections and, cumulatively, introduction of oscillatory component in turbine drive torque.

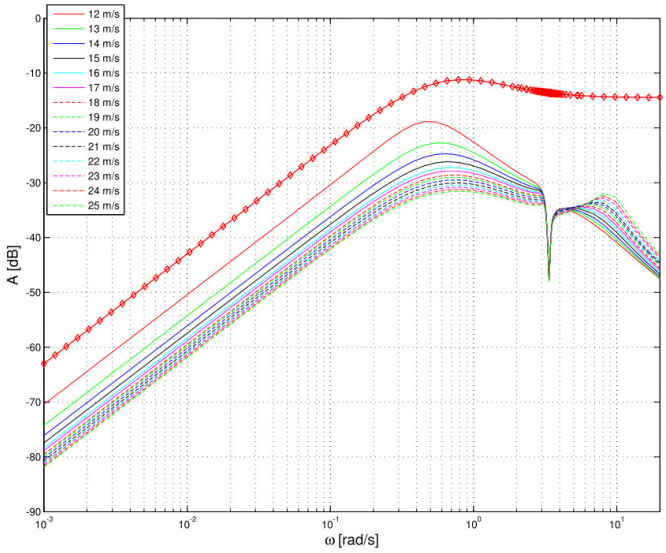

Fig. 16. Validation of disturbance specifications in frequency domain (boundary marked with red diamond markers)

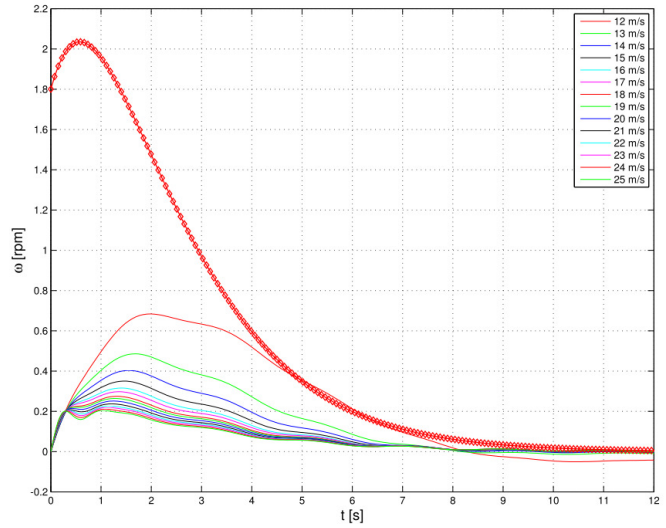

Fig. 17. Validation of disturbance specifications in time domain (boundary marked with red diamond markers)

So far validation was performed on family of linear models obtained by linearization of model given by (14) for wind speed ranging from 12 to 25 m/s. Plot on Fig. 18. confirms that given specifications have been satisfied even for nonlinear model. No particular differences are observed comparing validation performed on family of linear models and on nonlinear model. It is interesting to observe how the controller $C(s)$ behaves when faced with a simulation on a professional wind turbine simulation tool (Bladed, [8]) that also offers possibility of obtaining family of linear models of very high order (>40). This model besides the first and second mode of fore-aft movement, also includes equal number of side-side tower modes and rotor in-plane and out-plane modes that were neglected in simplified nonlinear model given by (14). The response of rotor speed and pitch

angle when performing simulations in Bladed is given on Fig. 19. It shows almost equal "main" dynamic of responses compared to responses of simplified nonlinear process. Response from Bladed contains though richer contents due to high order effects originating, among others, from in-plane and out-plane movement of blade sections in reference to their stationary position. Controller $C(s)$ would perform better if it was designed upon boundaries generated in reference to high order linear models obtained from Bladed. In this case an introduction of gain scheduling that reduces gain in high wind speed range would aid the controller and reduce the blade oscillatory movement thus reducing tear-and-wear.

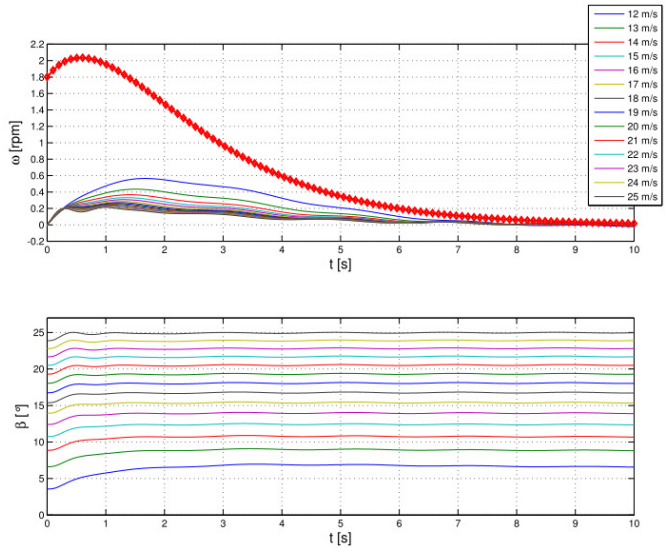

Fig. 18. Validation on nonlinear model

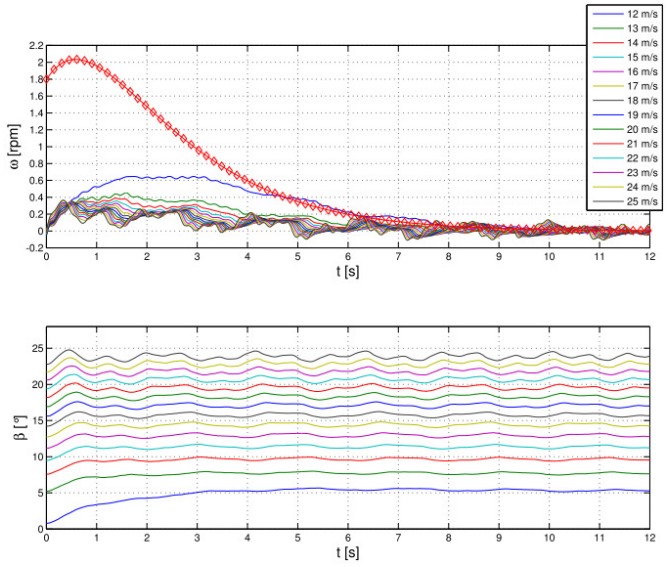

Fig. 19. Validation in Bladed

9. CONCLUSION

QFT proved to be an adequate method for synthesis of rotor speed controller despite existing variations in wind turbine dynamics. This should not come as a surprise as it was mentioned earlier that QFT had been very successfully integrated in helicopter and airplane control systems. Usually robust controllers are of high order but in this case, due to transparency of the QFT and its ability to explicitly address the uncertainty of wind turbine dynamics, an efficient controller of second order was obtained that uses no other aids (feedforward action, gain scheduling, etc.) to achieve specified closed loop behavior. Strong point of this method is also the ability it gives the user to perceive when the combination of process uncertainty and performance demands poses to big of an obstacle for chosen control structure. In this case it was possible to conclude that (judging by Bladed simulation results) introduction of gain reducing element scheduled on pitch angle would aid the performance of the controller in high wind regime thus obtaining a hybrid solution that combines adaptive and robust algorithms.

ACKNOWLEDGMENTS

This work was financially supported by Končar – Electrical Engineering Institute and the Ministry of Science Education and Sports of the Republic of Croatia.

REFERENCES

1. Damping of Wind Turbine Tower Oscillations through Rotor Speed Control. M. Jelavić, N. Perić, I. Petrović. Monaco : s.n., 2007. International Conference on Ecologic Vehicles & Renewable Energies.
2. T. Burton, D. Sharpe, N. Jenkins, E. Bossanyi. Wind energy handbook. s.l. : John Wiley and sons, 2001.
3. Modelling and control of variable-speed wind trubine drive-system dynamics. P. Novak, T. Ekelund, I.Jovik, B. Schmidtbauer. 4, 1995, Control system magazine, Vol. 15, pp. 28-33.
4. In memoriam – The life of prof. Isaac Horowitz. Chait, Y. i Jayasuriya, S. prosinac 2005, IEEE Control Systems Magazine.
5. Houpis, C.H., Rasmussen, J.R. i Garcia-Sanz, M. Quantitative Feedback Theory – Fundamentals and Application. 2. edition. Boca Raton : CRC Press, 2006.
6. E. L. van der Hooft, P. Schaak, T. G. van Engelen. Wind turbine control algorithms, Dowec WP1 - task 3 ECN-C-03-111. Petten, Netherlands : ECN Wind Energy, 2003.
7. F. D. Bianchi, H. De Battista, R.J. Mantz. Wind turbine control system, principles, modeling and gain scheduling design. s.l. : Springer, 2006.
8. Bossanyi, E. GH Bladed user's manual. Bristol : Garrad Hassan and Partners Limited, 2009.
9. Aranda J., Díaz J.A., Dormido S.,. SISO-QFTIT An interactive software tool for the design of robust controllers using the QFT methodology USER'S GUIDE. Madrid : U.N.E.D Departamento de Informática y Automática , 2005.
10. Borghesani, C., Chait, Y. and Yaniv, O. The QFT Frequency Domain Control Design Toolbox For Use with MATLAB. 3. izdanje. s.l. : Terasoft, Inc., 2003.
11. MIMOQCAD: a Mathematica based multivariable control system CAD package. Breslin, S.G., Grimble, M.J., Houpist, C.H. 1996. Symbolic Computation for Control (Digest No: 1996/078), IEE Colloquium on .
12. Identification of Wind Turbine Model for Controller Design. M. Jelavić, N. Perić, I. Petrović. Portorož, Slovenia :

s.n., 2006. Proceedings of the 12th International Power Electronics and Motion Control Conference. pp. 1608-1613.

Appendix A. QFT GUI

Although several tools exist that offer the possibility of interactive QFT controller design (see [9], [10], [11]), an attempt was made to implement a simple QFT tool within Matlab® environment. As a result QFT GUI application (see Fig. 20) was implemented which offers its user the possibility to define the process in a structure given by (18). Furthermore, sensor and actuator dynamics can also be selected. This test version of GUI enables defining of two types of specification that were used in this article (disturbance rejection, stability margin). Calculate button translates given specification on to the Nichols chart (in the form of open loop boundaries) where controller design commences. The controller is designed interactively as the effects of either movement, deletion or addition of zeroes and poles are seen on Nichols chart. At any point the user can validate quality of controller design in time and frequency domain. It is important to stress that the validation is performed on the user defined set of linear processes. It is up to user to validate if the controller design is adequate on a nonlinear process model.

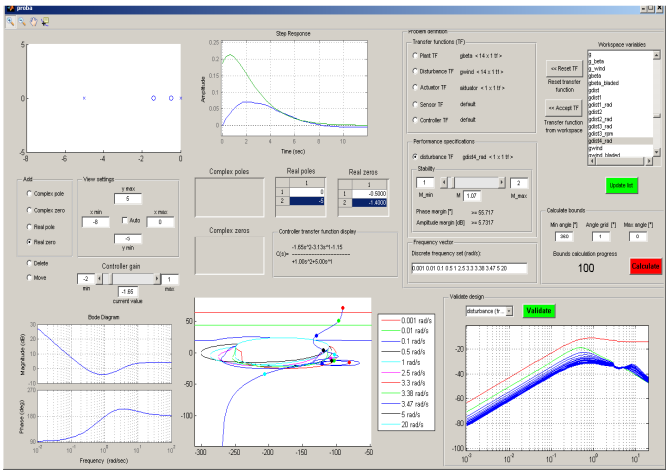

Fig. 20. QFT GUI application